Durability of PCL Nanocomposites Under Different Environments

A. Delgado-Lima - G. Botelho -
M. M. Silva - A. V. Machado

Abstract

The stability of PCL/TiO_2 nanocomposites under different environments was investigated. Samples were exposed to UV radiation in an accelerated weathering chamber equipment and characterized by viscosimetry and differential scanning calorimetry. The results showed that the presence of nanoparticles containing titanium enhanced polymer chain scission during UV exposure. For all samples, the melting temperature and crystallinity increased along photodegradation time. The biodegradability, assessed by biochemical oxygen demand, increased as the amount of inorganic particles increased. However, the thermal stability and activation energy evaluated by thermogravimetric analysis decreased as the amount of inorganic nanoparticles increased, indicating that nanocomposites exhibited lower thermal stability.

Keywords Poly(ε-caprolactone) - Nanocomposites Photodegradation · Biodegradation · Activation energy

Introduction

Polymers have been replacing conventional materials, as ceramics, metal and paper in packaging applications due to their functionality, processability, lightweight and low cost [1-3]. However, the development and research on polymeric materials resulted in very durable products with

tailor-made properties [1]. Thus, its use arise environmental problems related with waste management, leading to the implementation of some strategies, such as, landfills, plastic incineration and recycling [1, 4-6]. An alternative to these processes would be the development of biodegradable polymers with similar performance to conventional polymers, which requires modification to enhance its properties [4,6 – 10]. It has been shown that the addition of inorganic fillers, which can be dispersed at nanometric size, is a viable alternative to improve these materials properties [11, 12]. Biodegradable polymers, such as, polylactide (PLA), starch and poly(ε-caprolactone) (PCL) have been used as matrix [6, 7, 9, 13-19]. Therefore, in applications with short life-cycle, like packaging, the use of biodegradable nanocomposites seems to be an ecological alternative to reduce packaging waste [3,8,9]. Until now, the most used fillers for packaging applications are clays, rods and carbon nanotubes [15-19]. However, titanium particles have also being developed as fillers for packaging applications [11]. Moreover, titanium

dioxide (TiO_2), in the anatase crystal form, is very reactive and widely known for its photocatalytic action, since the presence of these particles enhances the photodegradation of the polymer matrix [11].

Several authors have already studied the degradation of biodegradable polymers and respective nanocomposites. Tsuji [20] and co-workers investigated the photodegradation of melt crystallized poly(l-lactide) (PLLA-C) and amorphous (PLLA-A) during 200 h . They found out that elongation to break (ε) decreased drastically. Sadi [21] noticed that during photodegradation poly(3-hydroxybutyrate) (PHB) both chain scission and crosslinking occurred, but the former prevailed. Recently Gardette [22] proposed a PLA degradation mechanism based on the formation of an anhydride. This mechanism involves a classical hydrogen abstraction on the polymeric backbone at the tertiary carbon in the α-position of the ester function leading to the formation of macroradicals. It is postulated that initiation of the photochemical reaction results from the presence of chromophoric defects in the polymer at very low concentrations.

Since there is a lack of studies on nanocomposites stability under different environments, the present study aims to investigate the durability of PCL/TiO_2 nanocomposites under the presence of UV radiation, microorganisms and temperature. Samples were placed in an accelerated weathering chamber, removed along exposure time and characterized by viscosimetry measurements and differential scanning calorimetry. Biodegradability was assessed by biochemical oxygen demand (BOD). The thermal stability, as well as, the activation energy was evaluated by thermogravimetric analysis.

Experimental Part

Materials

Poly(ε-caprolactone), CAPA FB100 ($M_n > 100{,}000$ g/ mol) supplied from Perstrop was used as a biodegradable polymer and titanium butoxide ($Ti(OBu)_4$), ($M_n = 340.027$ g/mol), from Aldrich was used as precursor.

Sample Preparation

Nanocomposites with 1 and 4% of titanium butoxide (TBT1 and TBT4) were prepared by melt mixing, using a batch mixer (Rheomix 6000S, volume 69 mL) at 90°C, rotor speed of 100 rpm during 8 min .

Films were made, from the samples previously prepared, in a hot press at 90°C and samples of $30 \times 120 \times 0.4$ mm (width × length × thickness) were cut by hand.

Photodegradation

The photodegradation tests of PCL, TBT1 and TBT4 samples were carried out in a Xenotest 150 S chamber equipped with a filtered xenon lamp with $60 Wm^{-2}$ of intensity, during a period of 700 h , according to standard procedures [23]. The Xenotest creates an

accelerated environment of the natural weathering process, in which the material will be exposed during its lifetime. It simulates daylight exposure with heat and humidity.

Biodegradation

Biodegradation was assessed in aqueous environment under aerobic conditions according to the standard ISO 14851:1999, which specify a method for the determination of biochemical oxygen demand (BOD) in a closed respirometer. The complete procedure is described in Moura [24].

Thermal Degradation

The thermal degradation kinetics was investigated taking into account the thermogravimetric data. A typical model for the thermal decomposition of a homogeneous system was used according to Eq. 1 [25]:

$$\frac{\partial \alpha}{\partial k} = k(T) f[\alpha(t)] \tag{1}$$

where, α is the degree of conversion of the sample under degradation, calculated by Eq. 2:

$$\alpha = \frac{w_0 - w_{(t)}}{w_0 - w_\infty} \tag{2}$$

where, $w_0, w_{(t)}$ and w_∞ are the sample weight before degradation, at time t and after complete degradation, respectively. The rate constant, $k(t)$, depends on the absolute temperature according to the Arrhenius equation. Since polymer degradation are often chain reaction $s, f(\alpha)$ represents the results of elementary steps. For solid state reactions, $f(\alpha) = (1-\alpha)^n$, where n is the reaction order, and it was assumed that it is constant during the degradation process. Therefore, the activation energy of the samples was determined by the Ozawa-Flynn-Wall (OFW) using several heating rates, 5,10,15 and 20°C/min, between 30 and 530 °C, under nitrogen atmosphere (60 mL/min) using a TA Q500 thermobalance. The samples were analyzed in duplicate. The TGA curve at each heating rate allows to estimate a temperature for a specific conversion level. The plot of the heating rates logarithm against the absolute temperature gives a straight line, which allows to assess the activation energy [26, 27]. The isoconversional method of OFW [28,29] is a method that uses Eq. 3, which assumes that the conversion function, $f(\alpha)$, does not change with the variation of the heating rate for all degree of conversion, α, values. It involves a temperature measurement corresponding to fixed values of α from the experiments at different heating rates (hr).

$$\ln(hr) = \ln \frac{AE_{act}}{R} - \ln f(\alpha) - \frac{E_{act}}{RT} \tag{3}$$

where, A is a pré-exponential factor (min^{-1}) and $\mathrm{E_{act}}$ is the activation energy (kJmol^{-1}).

This method is a powerful tool to study the degradation kinetics using thermogravimetric data obtained from complex processes, like thermal degradation of polymers and allows to evaluate the activation energy without a previous knowledge of the reaction order, which in many cases is a great advantage [30].

Characterization

Samples of 70 nm thickness were cut using a diamond knife, in a Leica ultramicrotome at −60°C. The cut sections were transferred onto copper grids and then analysed without stain in a Philips CM120 transmission electron microscope (TEM).

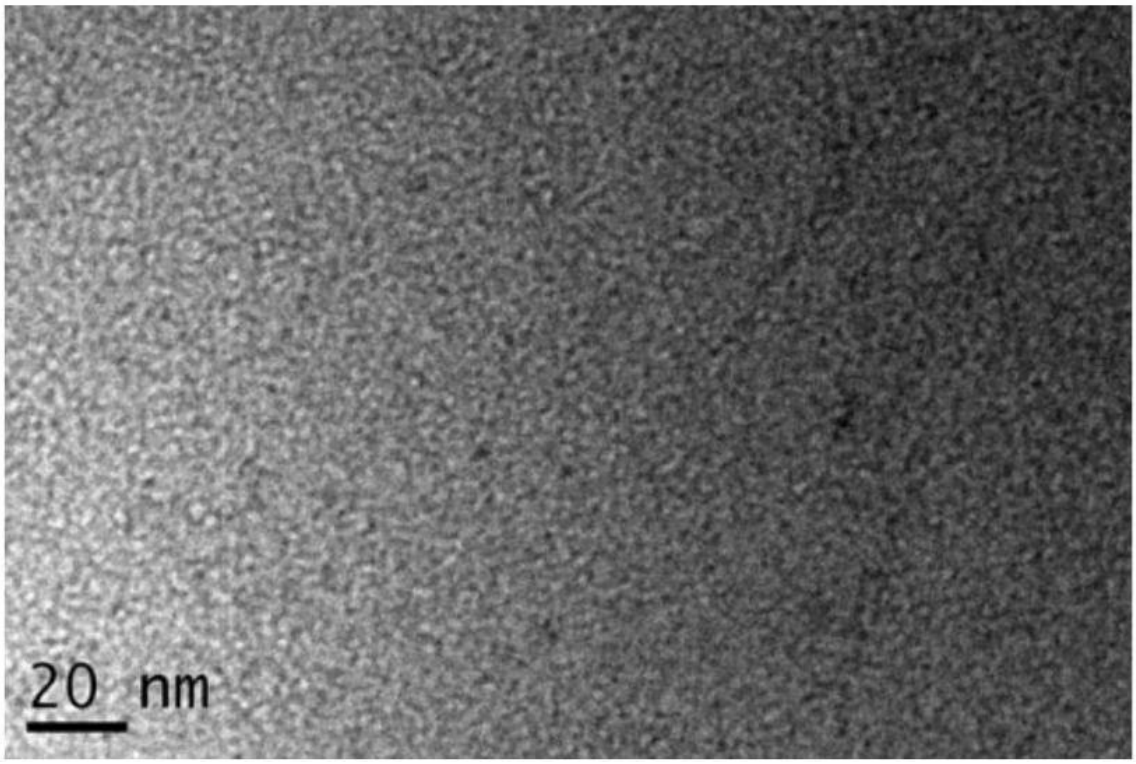

Fig. 1 TEM micrograph of TBT1 nanocomposite

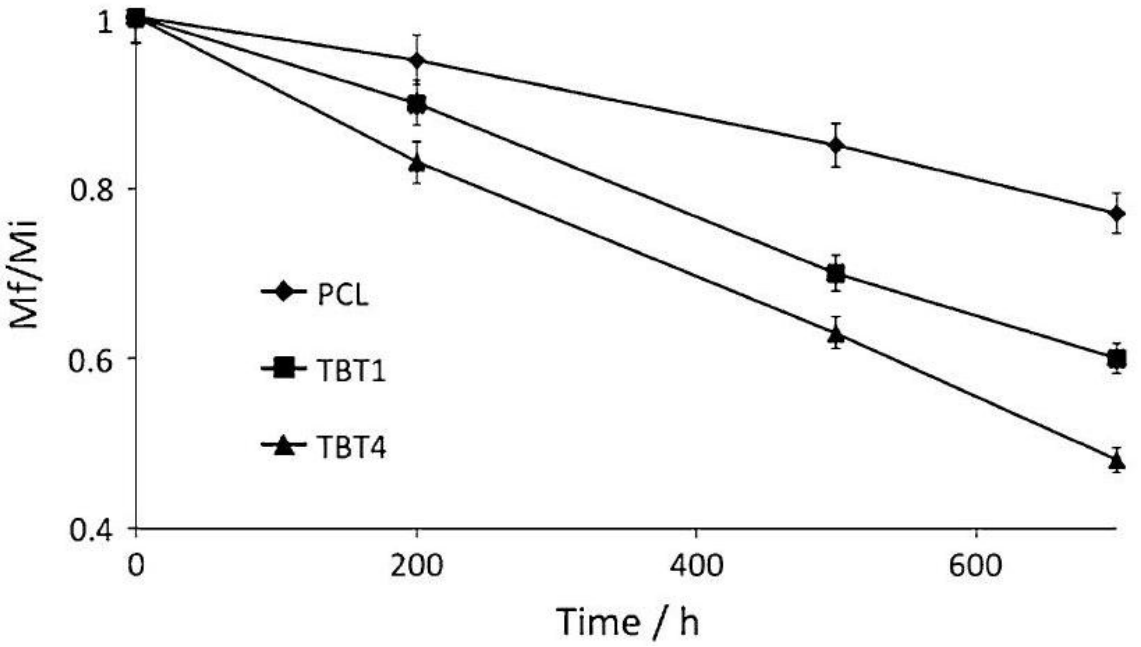

Fig. 2 Evolution of the molecular weight ratio of PCL, TBT1 and TBT4 samples along exposure time

The viscosity measurements were performed in a water bath at $25.0 \pm 0.1°C$ using an Ubbelohde type viscometer. Toluene was used as solvent and the concentration of each solution was around 0.002 g/mL. Four measurements were performed for each filtered solution. The viscosimetric molecular weight was determined through the Mark-Houwink equation [31].

Samples were analysed by differential scanning calorimetry under an argon atmosphere between 0 and 120°C, at a heating rate of $10\ °C min^{-1}$ using a Mettler DSC 821e. Two analyses were performed for each sample. The onset melting temperature (T_m) and crystallinity degree (χ) were determined from the first run. While the onset temperature was calculated by the equipment software, the crystallinity degree was determined using Eq. 4:

$$\chi(\%) = \frac{\Delta H_f(PCL \text{ samples})}{\Delta H_f^0(PCL)} \times 100 \quad (4)$$

ΔH_f was determined for each sample and the value of ΔH_f^0 of PCL was 139.5 J/g [13].

Results and Discussion

Figure 1 depicts, as an example, the morphology of TBT1 nanocomposite investigated by TEM, which shows a fine dispersion of inorganic particles with a few nanometers in the polymeric matrix.

The molecular weight ratio as a function of degradation time (0,200,500 and 700 h) for PCL, TBT1 and TBT4 nanocomposites is plotted in Fig. 2. Even though a decrease of molecular weight of the samples is clearly observed along the exposure time, it is more

significant for nanocomposites. These results clearly indicate that degradation of the polymer matrix along exposure time occurred by chain scission and was more pronounced when inorganic particles were presented [32]. This is in agreement

Fig. 3 DSC curve of the PCL samples before (line) and after photodegradation (square)

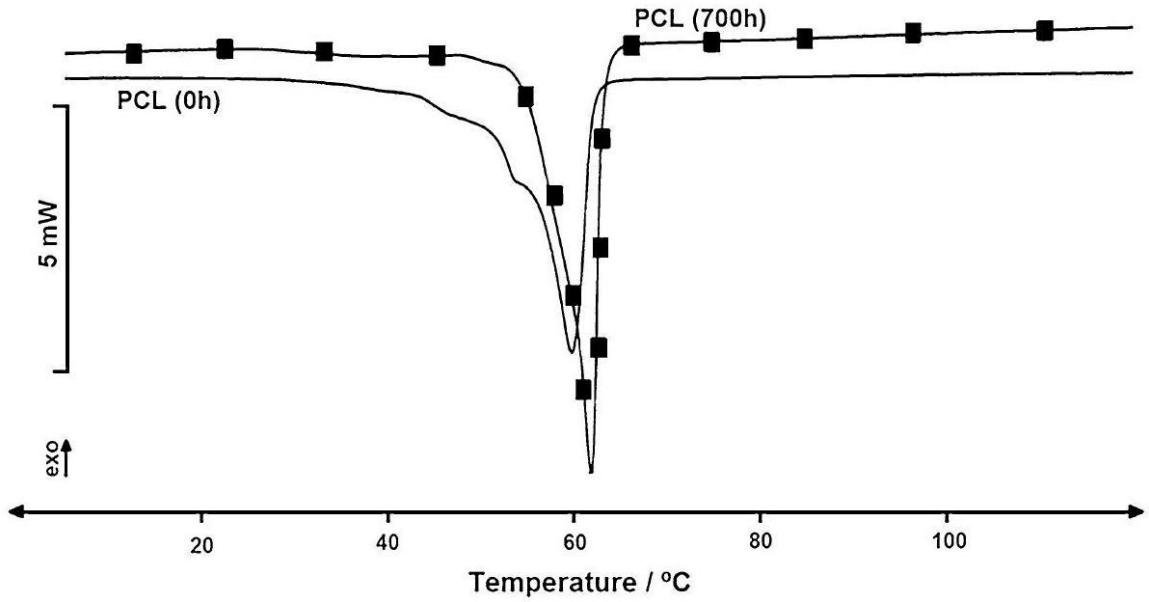

with the published PCL photodegradation mechanism that occurs by free radical process and leads to a breakdown of the polymer backbone via the Norrish II mechanism at the ester group and the sequential two methylene groups adjacent to the ester oxygen [20].

As expected, the slope rises as the amount of TBT increases, which indicates that the inorganic nanoparticles enhanced the polymer degradation due to its photocatalytic activity [33, 34]. In this case degradation was initiated both by UV radiation and nanoparticles containing titanium.

DSC curves of PCL and TBT4 samples before and after photodegradation are shown in Figs. 3 and 4. Non-degraded samples of PCL and TBT4 exhibit two melting peaks, which were attributed to the melting of the original crystals

Fig. 4 DSC curve of the TBT4 samples before (line) and after photodegradation (square)

Fig. 5 Onset melting temperature **a** and crystallinity degree **b** of PCL, TBT1 and TBT4 before and after photodegradation

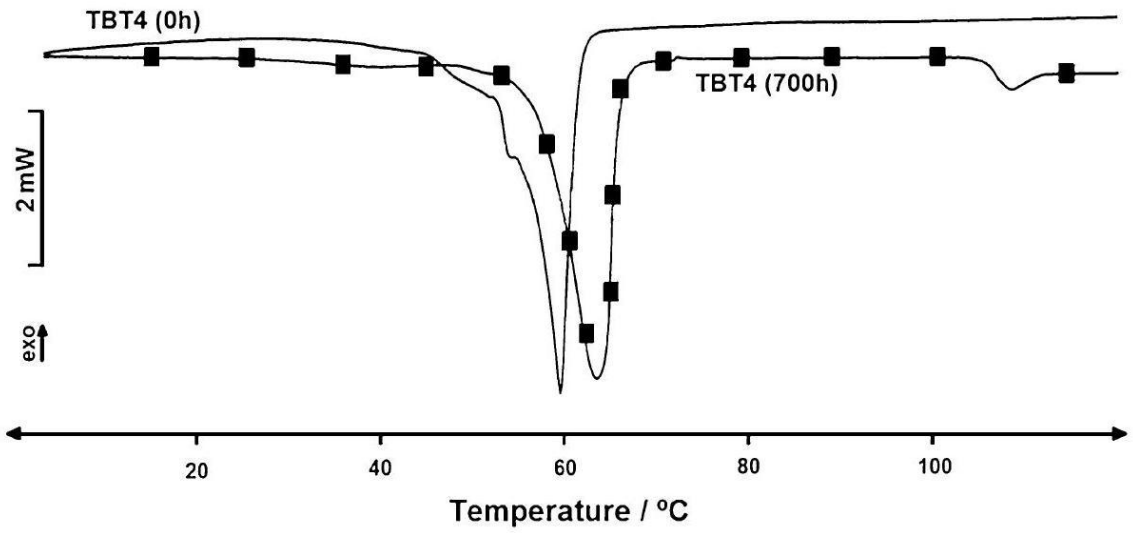
TBT4 (0h)
TBT4 (700h)
2 mW
exo
20
40
60
80
100
Temperature / ºC

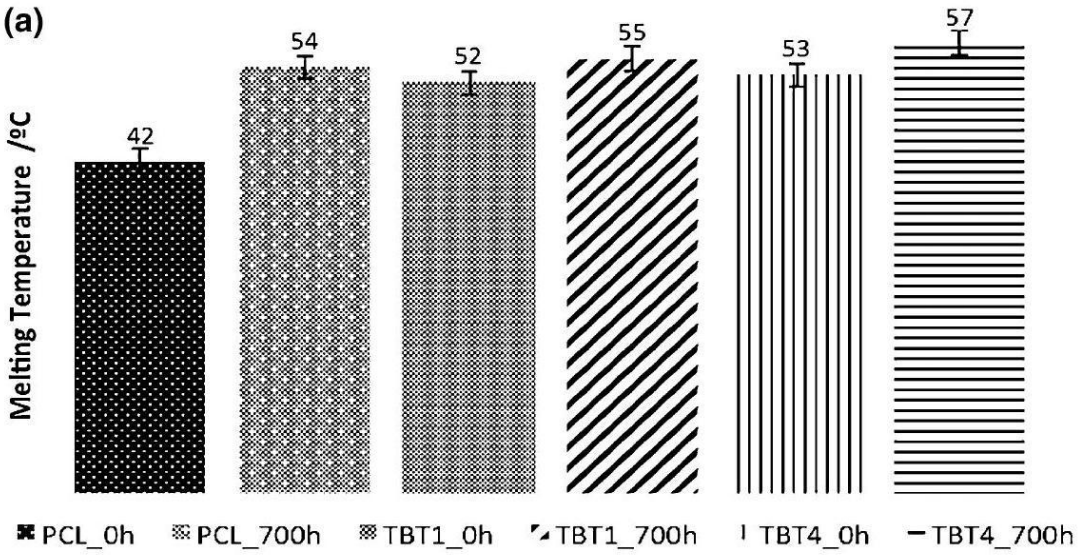
(a)
Melting Temperature /ºC
42
54
52
55
53
57
PCL_0h
PCL_700h
TBT1_0h
TBT1_700h
TBT4_0h
TBT4_700h

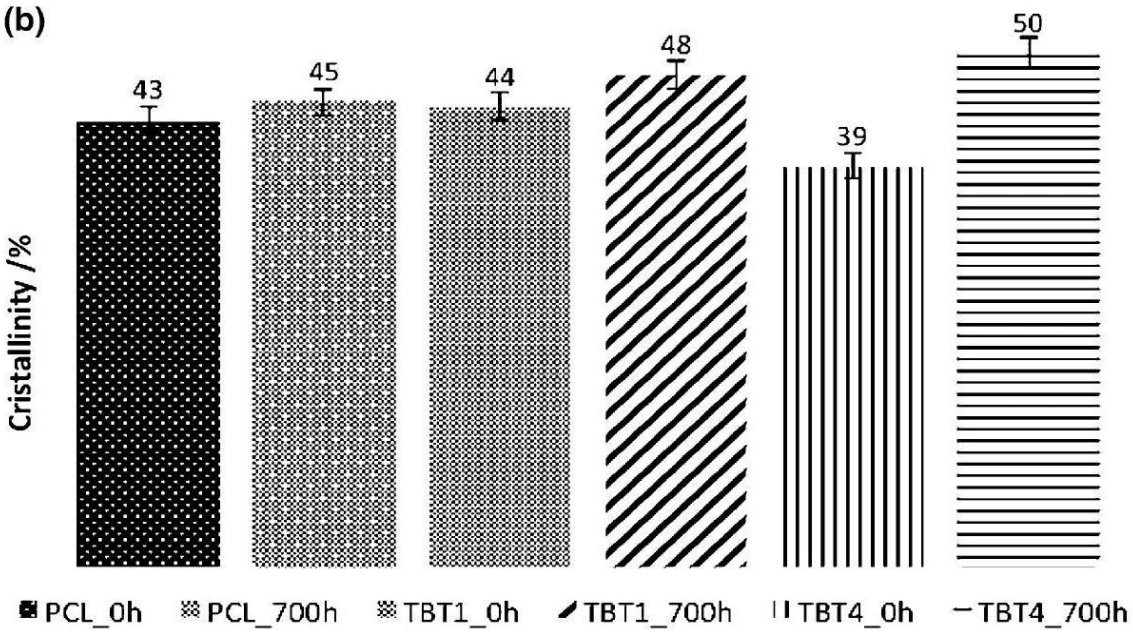
(b)
Cristallinity /%
43
45
44
48
39
50
PCL_0h
PCL_700h
TBT1_0h
TBT1_700h
TBT4_0h
TBT4_700h

Fig. 6 Biodegradability of PCL and nanocomposites according to ISO 14851

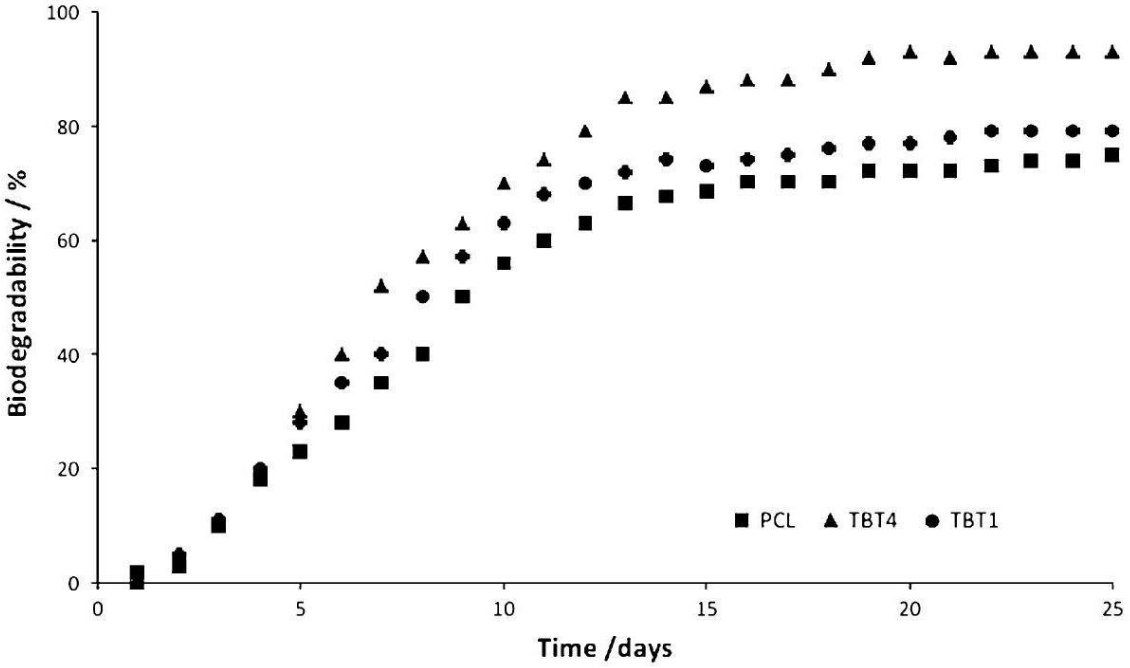

er degradation, in both
ved. Moreover, com-
f photodegradation the
eratures. This can be
rystallites in PCL film
sence of nanoparticles
s the melting temper-
ed by the interactions
c nanoparticles.
t melting temperature
ples before and after

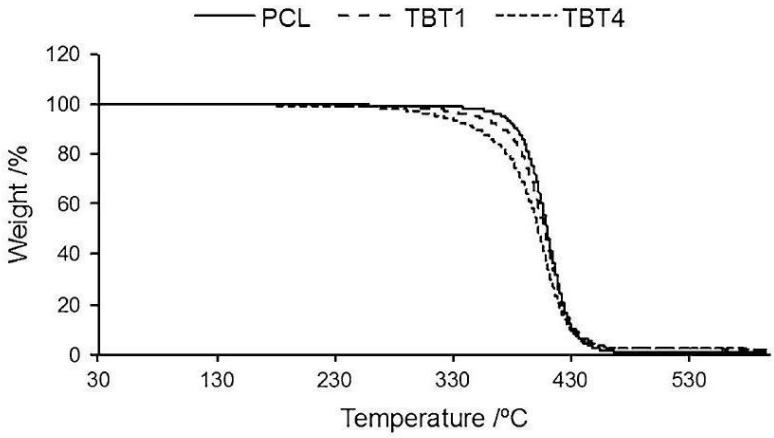

Fig. 7 TGA curves of PCL, TBT1 and TBT4 obtained at $10^{\circ}\mathrm{C}\,\mathrm{min}^{-1}$

As it can be observed in Fig. 7, PCL completely degrades till about 430°C. The onset temperature of the samples (390, 384 and 375 for PCL, TBT1 and TBT4, respectively) indicates that samples containing inorganic nanoparticles exhibit lower thermal stability than PCL, which decreased as the amount of nanoparticles increased. The lower thermal stability of the nanocomposites can be due to the presence of the organic part of the precursor (TBT), which has a low boiling temperature and volatilizes at lower temperature.

Figure 8 presents, as an example, the TGA curves of PCL obtained at 5,10,15 and $20^{\circ}\mathrm{C}\,\mathrm{min}^{-1}$, respectively. As the heating rate decreases the onset temperature decreases.

This result is due to the fact that lower heating rates allow a better homogenization of the phenomena that happens in the material during heating, once the material has higher response time.

The isoconversional OFW method, Eq. 3, was applied to calculate the activation energy of PCL, TBT1 and TBT4 samples at different conversions values, from the linear fitting of log hr versus 1/T (Fig. 9). In the present study, the conversion rates values used were 0.6, 0.7, 0.8 and 0.9. The

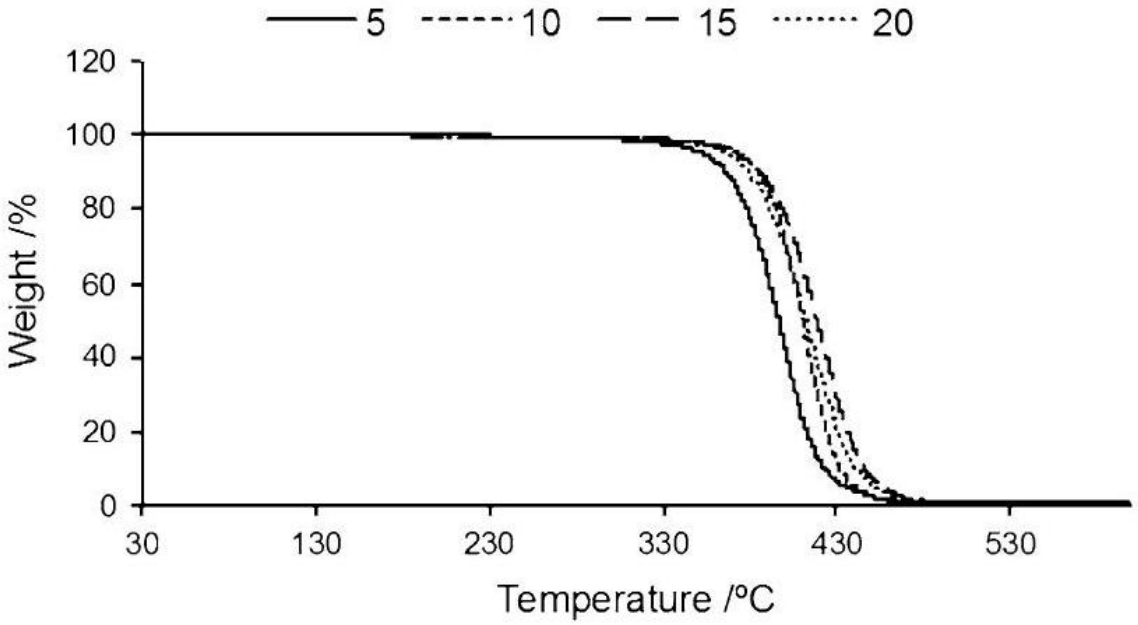

Fig. 8 TGA curves of PCL obtained at 5,10,15 and 20°Cmin $^{-1}$

OFW plots of the samples with a correlation coefficient of $R > 0.90$ are presented in Fig. 9. The fitting straight lines are nearly parallel, which indicate that this method can be applied to PCL and nanocomposites in the conversion range studied. The activation energy obtained for each conversion level is shown in Fig. 10. A change in the activation energy was observed as the conversion rate increased, which suggests the existence of a complex decomposition mechanism [36]. If the calculated values were the same for various values of α, it could be concluded that the degradation occurs through a single stage mechanism. On contrary, a change of E_{act} as the conversion degree increases indicates a complex reaction mechanism that invalidates the separation of the variables involved in the OFW analysis [37, 38]. Therefore, the increase in the activation energy along conversion level (Fig. 10) indicates that the kinetics can only be interpreted in terms of multistage degradation mechanism [39, 40].

The average activation energy is higher for PCL and decreases as the TBT amount increases (Fig. 11). This result can be explained by the titanium photocatalytic activity, which is responsible for the faster degradation of the polymer matrix by chain scission. Therefore, the

Fig. 9 Plots of the logarithm of the heating rate versus reciprocal temperature of the **a** PCL and **b** TBT4, for various conversion levels

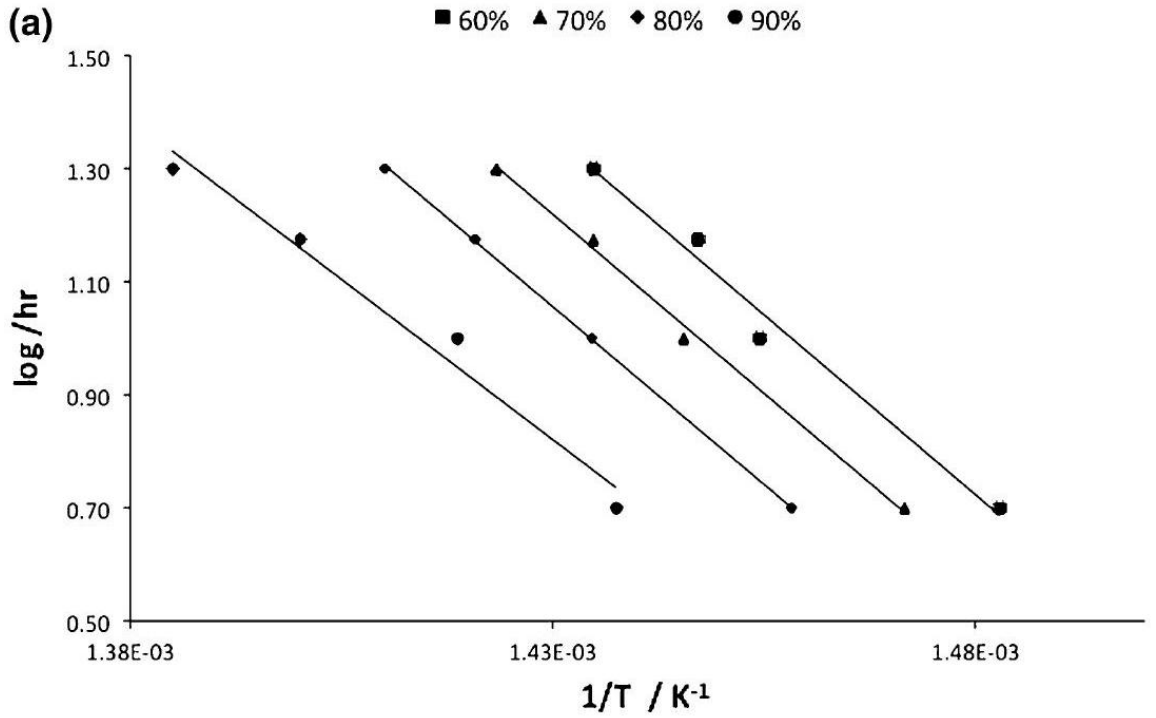

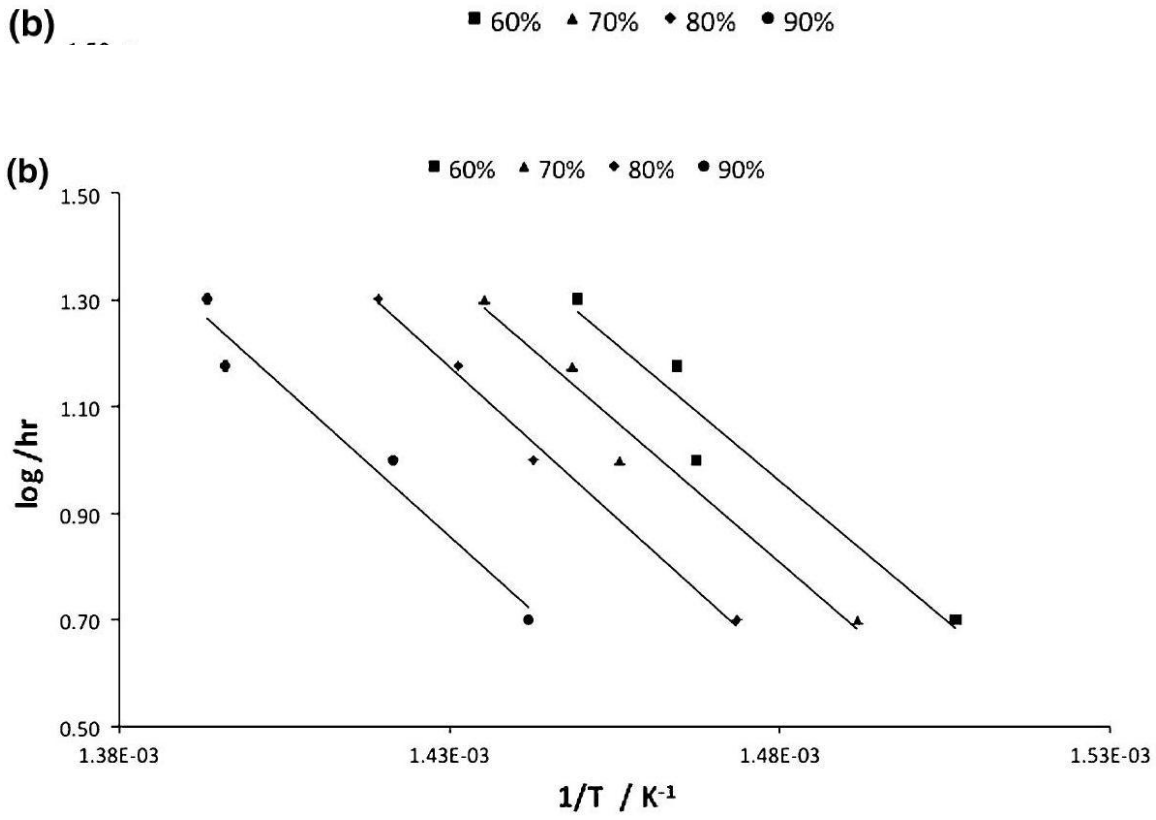

Fig. 10 Activation energy versus conversion level

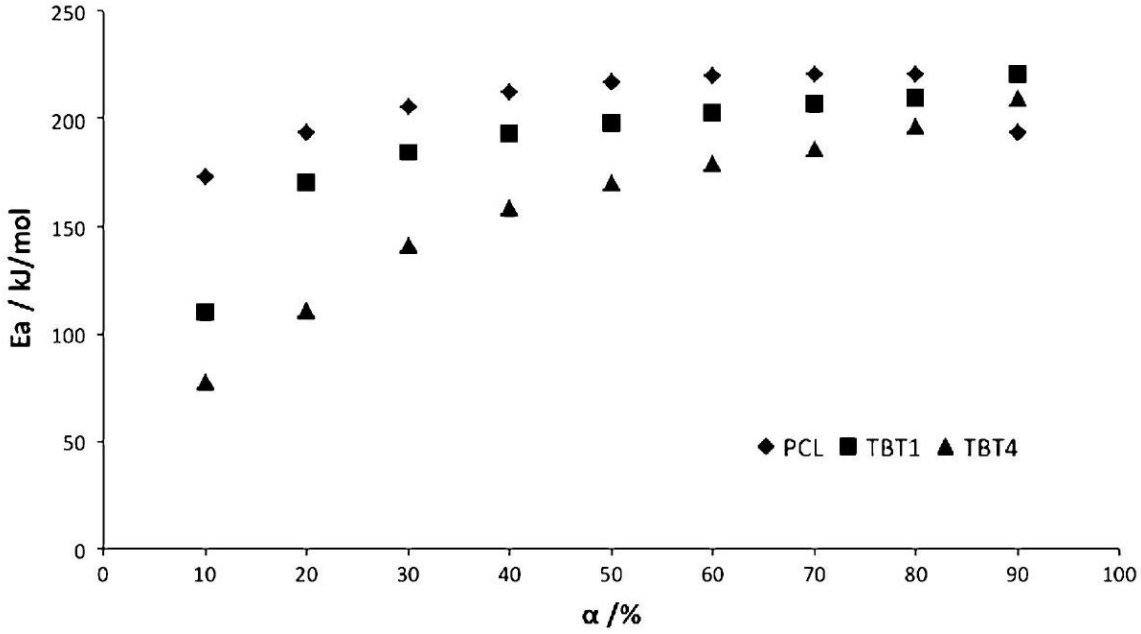

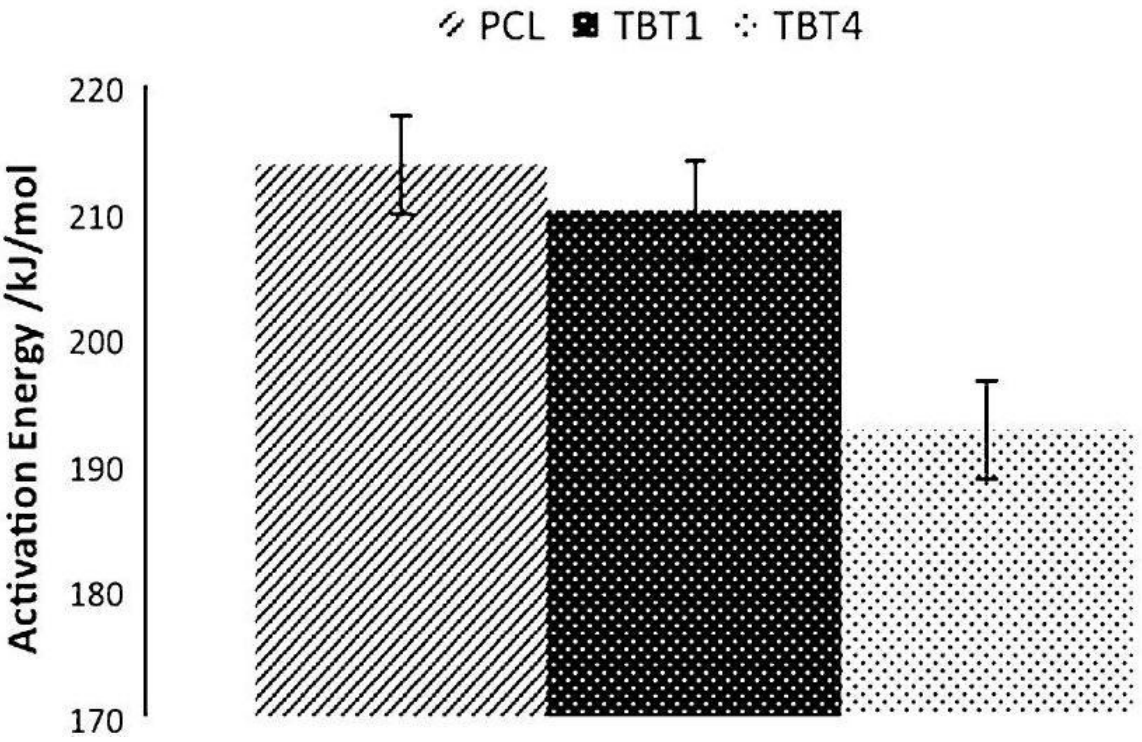

Fig. 11 Samples activation energy samples with higher titanium amount need less energy to degrade, i.e., the activation energy of these samples is always lower than for the polymer matrix.

Conclusions

The stability of PCL/TiO2 nanocomposites under different environments was investigated.

During the photodegradation study the chain scission phenomena was responsible for the molecular weight decrease. The thickening of the crystallites caused by UV irradiation and the higher flexibility of the smaller macromolecular chains promoted by chain scission, result in an increase of the samples crystallinity and melting temperature.

As it was expected due to the photocatalytic activity of the titanium, PCL showed higher activation energy than nanocomposites. The change in the activation energy with the conversion level, suggest the existence of a multi-stage degradation mechanism.

The nanocomposites prepared exhibited higher biodegradability but lower photo and thermal stability than PCL, which would be suitable for packaging applications.

Acknowledgments The authors acknowledge the financial support given by FCT through the project PTDC/AMB/73854/2006. FCT and FEDER (European Fund for Regional Development)-COMPETE-QREN-EU for financial support to the Research Centre, CQ/UM-PEst-C/QUI/UI0686/2011 and I3N-PEst-C/CTM/LA0025/2011 (FCOMP-01-0124-FEDER-022716).

References

1. Matthews FL, Rawlings RD (1994) Composite materials: engineering and science. Chapman and Hall, London
2. Amit A, Padua GW (2010) J Food Sci 71: 43
3. Azeredo HMC (2009) J Food Res Int 42: 1240
4. Shirai MA, Grossmann MVE, Mali S, Yamashita F, Garcia PS, Müller CMO (2013) Carbohydrate Polym 92:19
5. Silva RV, Brito J, Saikia N (2013) Cem & Conc Composites 35:23
6. Fukushima K, Abbate C, Tabuani D, Gennari M, Rizzarelli P, Camino G (2010) Mat Sci Eng C 30:566
7. Fukushima K, Tabuani D, Camino G (2009) Mat Sci and Eng C 29:1433
8. Bang G, Kim SW (2012) J Ind Eng Chem 18:1063
9. Gorrasi G, Milone C, Piperopoulos E, Lanza M, Sorrentino A (2013) J Applied Clay Sci 71:49
10. Vroman I, Tighzert L (2009) Materials 2:307
11. Nguyen VG, Thai H, Mai DH, Tran HT, Tran DL, Vu MT (2013) Composites B 45:1192
12. Jayaramudu T, Raghavendra GM, Varaprasad K, Sadiku R, Raju KM (2013) Carbohydrate Polym 92:2193

13. Botelho G, Silva MM, Neves IC, Fonseca AM, Machado AV (2011) J Polym Res 18:1743
14. Moura I, Botelho G, Machado AV (2013) J Polym Environ submitted
15. Román MSS, Holgado MJ, Salinas B, River V (2013) J Applied Clay Sci 71:1
16. Haldorai Y, Shim JJ, Lim KT (2012) J Supercritical Fluids 71:45
17. Luo YB, Wang XL, Wang YZ (2012) Polym Degrad Stab 97:721
18. Rakovsky A, Gotman I, Rabkin E, Gutmanas EY (2013) J Mech behav Biomedical Mat 18:37
19. Najafi N, Heuzey MC, Carreau PJ (2012) Composites Sci Tech 72:608
20. Tsuji H, Echizen Y, Nishimura Y (2006) Polym Degrad Stab 91:1128
21. Sadi RK, Fechine GJM, Demasquette NR (2010) Polym Degrad Stab 95:2318
22. Gardette M, Thérias S, Gardette JL, Murariu M, Dubois P (2011) Polym Degrad Stab 96:616
23. ISO 4892-2 (2006) Plastics-Methods of exposure to laboratory light sources-Part 2: Xenon-arc lamps
24. Moura I, Machado AV, Duarte FM, Nogueira R (2011) J Appl Polym Sci 119:3338
25. Sencadas V, Costa CM, Botelho G, Caparrós C, Ribeiro C, Gómez-Ribelles JL, Lanceros-Mendez S (2012) J Macromolecular Sci B 51:411
26. Machado AV, Neves IC, Botelho G, Rebelo P (2006) Mat Sci Forum 514-516:901
27. Neves IC, Botelho G, Machado AV, Rebelo P (2007) J Mater Chem Phys 104:5
28. Flynn JH, Wall LA (1966) J Polym Sci B 4:323
29. Ozawa T (1965) Bull Chem Soc Japan 38:1881
30. Hamciuc C, Vlad-Bubulac T, Petreus O, Lisa G (2007) Eur Polym J 43:980
31. Schindler A, Hibionada YM, Pitt CG (2003) J Polym Sci: Polym Chem 20:319
32. Kijchavengkul T, Auras R, Rubino M, Ngouajio M, Fernandez RT (2008) J Chemosphere 71:1607
33. Cho S, Choi W (2001) J Photochem Photobiol A Chem 143:221
34. Kim SH, Kwak S, Suzuki T (2006) Polym 47:3005
35. Li R, Nie K, Shen X, Wang S (2007) J Mat Letters 61:1368
36. Vyazovkin S, Sbirrazzuoli N (2006) Macromolecular Rapid Commun 27:1515
37. Chrissafis K, Paraskevopoulos KM, Bikiaris DN (2006) Polym Degrad Stab 91:60
38. Chrissafis K, Paraskevopoulos KM, Bikiaris DN (2005) Thermochim Acta 435:142
39. Babanalbandi A, Hill DJT, Hunter DS, Kettle L (1999) Polym Int 48:980
40. Aoyagi Y, Yamashita K, Doi Y (2002) Polym Degrad Stab 76:53